HHS Public Access

Author manuscript

Nature. Author manuscript; available in PMC 2019 February 26.

Published in final edited form as:

Nature. 2018 August ; 560(7717): 228–232. doi:10.1038/s41586-018-0385-7.

Shared evolutionary origin of vertebrate neural crest and cranial placodes

Ryoko Horie[#1], **Alex Hazbun**[#1], **Kai Chen**[#1], **Chen Cao**[1], **Michael Levine**[1,2,*], and **Takeo Horie**[1,3,*]

[1]Lewis-Sigler Institute for Integrative Genomics, Princeton University, Princeton, NJ, 08544, USA.

[2]Department of Molecular Biology, Princeton University, Princeton, NJ, 08544, USA.

[3]Shimoda Marine Research Center, University of Tsukuba, Shimoda, Shizuoka, 415-0025, Japan.

[#] These authors contributed equally to this work.

Placodes and neural crest represent defining features of vertebrates, yet their relationship remains enigmatic despite extensive investigations[1–3]. In this study we use a combination of lineage tracing, gene disruption, and single cell RNA-seq assays to explore the properties of the lateral plate ectoderm of the proto-vertebrate, *Ciona intestinalis*. There are striking parallels in the patterning of the lateral plate in *Ciona* and the compartmentalization of the neural plate ectoderm in vertebrates[4]. Both systems exhibit sequential patterns of *Six1/2*, *Pax3/7* and *Msxb* expression that depend on a network of inter-locking regulatory interactions[4]. In *Ciona*, this compartmentalization network produces distinct but related sensory cell types that share similarities with derivatives of both cranial placodes and neural crest in vertebrates. Simple genetic perturbations result in the inter-conversion of one sensory cell type into another. Particular efforts focused on the bipolar tail neurons (BTNs) since they arise from tail regions of the lateral plate and possess properties of dorsal root ganglia, a derivative of neural crest in vertebrates[5]. Strikingly, BTNs are readily transformed into PSCs (palp sensory cells), a proto-placodal sensory cell type arising from the anterior-most regions of the lateral plate in the *Ciona* tadpole[6]. Proof of transformation was confirmed by whole-embryo single cell RNA-seq assays. These findings suggest that compartmentalization of the lateral plate ectoderm preceded the advent of the vertebrates,

[*]Correspondence: Michael Levine, Lewis-Sigler Institute for Integrative Genomics, Princeton University, Princeton, NJ 08544, USA. msl2@princeton.edu. Takeo Horie, Shimoda Marine Research Center, University of Tsukuba, Shimoda, Shizuoka 415-0025, Japan. horie@shimoda.tsukuba.ac.jp.

Author contributions T.H., A.H., and M.L conceived the project. T.H., K.C., and M.L. designed the experiments. R.H., K.C., and T.H. performed the experiments. R.H., A.H., K.C., C.C., T.H. and M.L. analyzed and interpreted the data. T.H., A.H. K.C., C.C., and M.L. wrote the paper.

Competing interest
The authors declare no competing interest

Image acquisition. Images of transgenic larvae were obtained with a Zeiss AX 10 epifluorescence microscope.

Data availability. Single-cell RNA-seq data that support the findings of this study have been deposited in Gene Expression Omnibus (GEO) with the accession code GSE115331 (https://www.ncbi.nlm.nih.gov/geo/query/acc.cgi?acc=GSE115331). All other data support the findings of this study are available from corresponding author upon reasonable request.

and served as a common source for the evolution of both cranial placodes and neural crest [3,4].

Placodes and neural crest are the key ontogenetic novelties underlying vertebrate cephalization[1–3]. However, their evolutionary origins remain uncertain despite recent evidence that invertebrate chordates contain rudiments of both cell types[4–14]. Here we sought to obtain a more comprehensive view of the lateral plate ectoderm in *Ciona* since it is the source of the cell types that are related to placodal and neural crest derivatives in vertebrates.

Lineage-tracing methods were used to identify four derivatives of the lateral plate ectoderm: palp sensory cells (PSCs) arising from the a8.20 and a8.18 lineages[12], aATENs (a8.26 lineage)[14], pATENs (b8.20 lineage)[9] and BTNs (b8.18 lineage)[5] (summarized in Fig. 1a,b; Extended data Fig. 1). The aATENs were previously shown to possess dual properties of placode-derived chemosensory neurons (e.g., olfactory neurons) and GnRH-expressing neurosecretory neurons (e.g., hypothalamic GnRH neurons)[14]. The BTNs are thought to share properties with neural crest-derived dorsal root ganglia[5].

A regulatory “blueprint” of the *Ciona* embryo identified several determinants of the lateral plate ectoderm, including *Dmrt.a*, *Foxc*, *Six1/2*, *Pax3/7* and *Msxb*[15]. *Dmrt.a*, *Foxc*, and *Six1/2* are expressed in the anterior-most regions (a8.20 and a8.18 and a8.26 lineages) (summarized in Fig. 1c,d)[12,14,16], while *Msxb* is selectively expressed in posterior regions (b8.20 and b8.18 lineages) (Fig. 1d)[15,17]. *Pax3/7* straddles anterior and posterior regions, spanning the a8.26, b8.20, and b8.18 lineages (Fig. 1c)[18].

We have obtained evidence for inter-locking regulatory interactions among these lateral plate determinants (Fig. 2a-d; Extended Data Figs. 2-5). *Dmrt.a* activates *Foxc* and *Six1/2* expression in the anterior-most regions (Fig. 2a,b)[15,16]. There is an expansion of *Six1/2* and *Eya* expression into tail regions of *Msxb* morpholino (MO) morphants, suggesting that *Msxb* functions as a repressor to delineate the trunk/tail boundary of the lateral plate ectoderm (Fig. 2a-c; Extended Data Fig. 2). The characterization of a minimal *Six1/2* enhancer is consistent with direct repression by *Msxb* (Extended Data Fig. 4). Furthermore, there is an anterior expansion of *Msxb* expression in *Dmrt.a* MO morphant mutants, raising the possibility of reciprocal repression of *Msxb* by either *Six1/2* (and *Eya*) or *Dmrt.a* (Extended Data Fig. 5).

There are striking parallels in the compartmentalization of the lateral plate in vertebrates and ascidians (summarized in Fig. 1c). In *Xenopus*, *Dmrt.a* homologs 4 and 5 specify the adenohypophyseal/olfactory placodes within anterior regions of the pan-placodal primordium[19,20]. They do not appear to regulate *Six1* as seen in ascidians. Nonetheless, in *Ciona Dmrt.a* gives way to sequential expression of *Six1/2* and *Msxb* at the trunk/tail boundary, similar to that seen in vertebrates (Fig. 1c,d). Moreover, the overlapping patterns of *Six1/2* and *Pax3/7* expression seen for the *Ciona* aATEN lineage are evocative of those that delineate specific compartments within the pan-placodal primordium in vertebrates[21–23].

The most significant deviation in the *Ciona* and vertebrate regulatory fate maps is the compartmentalization of the *Ciona* anterior lateral plate into two distinct domains exhibiting mutually exclusive expression of *Foxc* (PSCs) and *Six1/2* (aATENs) (Fig. 1c, d). We sought to determine whether these territories might share common developmental properties since vertebrate orthologs of *Foxc* have been implicated in delineating placodal derivatives such as the eye lens[24–26]. *Foxc* morphants were obtained by injection of a sequence-specific MO targeting the translation start site of the endogenous *Foxc* gene. They show a loss of PSC marker gene expression (Fig. 2e,f) as well as an unexpected phenotype: ectopic expression of a *Six1/2* reporter gene in palp regions producing PSCs (Fig. 2d,g,h; Extended Data Fig. 6). Thus, *Foxc* appears to function as a key determinant of PSC identity by activating PSC markers and inhibiting an alternate aATEN identity. This transformation of PSCs into aATENs suggests that the *Foxc* and *Six1/2* territories of the anterior lateral plate employ a similar developmental program for specifying sensory cells.

It has been suggested that the BTNs are related to dorsal root ganglia, which are derived from neural crest cells in vertebrates[5]. This observation raises the possibility that tail regions of the lateral plate ectoderm possess “proto-neural crest” properties[5], hinting to a common origin of cranial placodes and neural crest from lateral plate ectoderm[1]. To explore this possibility we asked whether BTNs could be transformed into other derivatives of the lateral plate ectoderm. Towards this goal we misexpressed *Foxc* in posterior regions of the lateral plate using *Pax3/7* and *Msxb* regulatory sequences. Mutant tailbud embryos display variable transformations of BTNs into PSCs (Fig. 2i-k) without altering other tail structures (e.g. neural tube and notochord). Some BTNs express only PSC marker genes (e.g. *βγ-crystallin*) (arrow, Fig. 2j) while others express both PSC and BTN markers (e.g., *Asic1b*) (arrowhead, Fig. 2j,k). These observations suggest that anterior and posterior regions of the lateral plate ectoderm employ a similar developmental program for the specification of related but distinct sensory cell types. It is therefore possible that the entire lateral plate of the last shared tunicate/vertebrate ancestor is the source of both placodal and neural crest derivatives in vertebrates.

Since the transformation of BTNs into supernumerary PSCs is pivotal to our proposal that the compartmentalized lateral plate ectoderm produces distinct but related sensory cell types, we employed single cell RNA-seq assays to characterize transformed BTNs by taking advantage of the well-defined lineages and small cell numbers comprising *Ciona* tailbud embryos (~1500 cells). Embryos were injected with the *Pax3/7>Foxc* transgene (Fig. 2j), grown to the late tailbud stage, dissociated and sequenced using the 10x microfluidics platform. Approximately 5000 cells were sequenced in order to obtain sufficient coverage (~3×) to ensure reliable detection of PSCs, BTNs, and transformed cell types. Unequivocal identification of cells expressing the *Pax3/7* transgene was provided by the insertion of a unique 450 bp sequence tag positioned downstream of the *Foxc* coding region.

tSNE projections reveal 20 cell clusters representing different tissues, including notochord, endoderm, tail muscles, mesenchyme, epidermis, and CNS (Fig. 3a; Extended Data Fig 7a,b and Supplementary Table1). BTNs were identified by their expression of key marker genes such as *Asic1b* and *synaphin*, while PSCs express a distinct set of markers including *Islet*, *SP8* and *Foxg* (Fig. 3b; Extended Data Fig. 7c, Fig. 8 and Supplementary Table1).

Transformed BTNs are defined as those expressing the *Pax3/7* transgene, lacking expression of BTN markers (*Asic1b* and *synaphin*), acquiring expression of PSC markers (*Islet, Foxg* and *SP8*), and clustering within the 95% confidence interval (CI) ellipse of native PSCs (bottom oval, Fig. 3c). Partially transformed BTNs are defined as those expressing *Pax3/7* transgenes, lacking expression of just one of the BTN marker genes, and acquiring expression of just a subset of PSC markers. The transcriptomes of hybrid cells tend to map outside the 95% CI ellipse of PSCs (Fig. 3c). Altogether, 45 BTNs were identified in the whole-embryo single cell transcriptome datasets. About half (21) are untransformed and display the native BTN transcriptome profile, while the other half are either fully transformed into PSCs (10) or partially transformed (14) into a hybrid BTN/PSC identity (Fig. 3d). These findings closely mirror the direct visualization of reporter gene expression in transgenic embryos, whereby BTNs exhibit variable expression of *βγ-crystallin* and *Asic1b* reporter genes (Fig. 2j,k).

The *Pax3/7>Foxc* transgene is expressed in the lateral plate and additional tissues, such as the mesenchyme, which is a common site of ectopic expression of *Ciona* transgenes[27]. These other sites of *Foxc* expression do not undergo transformations in cell identity, but instead display native transcriptome profiles (Extended Data Fig. 7e,f). Altogether, the single cell RNA-seq assays strengthen the evidence that BTNs are transformed into PSCs, suggesting the use of a similar developmental program for the specification of different sensory cells arising from head, trunk, and tail regions of the lateral plate ectoderm.

We have presented evidence that the antero-posterior compartmentalization of the *Ciona* lateral plate leads to the development of related but distinct sensory cell types (summarized in Fig. 4). PSCs, aATENs, and BTNs express a common suite of regulatory gene and cell identity genes (e.g., *POU IV, DCDC2* and *14–3-3ε*), despite their different origins along the lateral plate (Extended Data Fig. 9). *Foxc*, *Six1/2* and *Msxb* impose distinctive signatures of gene activity leading to the specification of diverse sensory cell types. There are striking parallels with the regional specification of distinct somatosensory neurons arising from placodal and neural crest territories in vertebrates[28]. We therefore suggest that a compartmentalized lateral plate preceded the advent of the vertebrates, and served as a common source for the evolution of both cranial placodes and neural crest.

SUPPLEMENTARY INFORMATION

METHODS

Biological Materials.—Wild-type *Ciona intestinalis* adults were obtained from M-Rep (San Diego, CA) and the National Bio-Resource Project for *Ciona* in Japan. Sperm and eggs were collected by dissecting the sperm and gonadal ducts.

Constructs.—Reporter genes were designed using previously published enhancer sequences: *Dmrt.a*[30], *Msxb*[17,31,32], *Six1/2*[14], *GnRH*[14], *CNGA*[14], *Foxc*[12], *Islet*[6]. The *Eya* (Ciinte.REG.KhC7:6052317–6053527) and *Pax3/7* (Ciinte.REG. KhC10:876118–879610) enhancers were isolated via PCR using the following primers (5’-atgcctgcagactcaattaccgaattaatt-3’ and 5’-gatcggatccatatttccatcacgaacttt-3’ for *Eya*, 5’-

atgcctgcaggtatgactgtgtaaatctgc-3’ and 5’-gatcggatccgtttgttgggttgtgttcag-3’ for *Pax3/7*) and cloned into the PstI/BamHI restriction site of the pSPeCFP vector.

The following fusion genes were used in the experiments presented in Extended Data Figure 9. For *Dmrt.a ΔMO target sequence* (Ciinte.REG.KhS544:4,240–5,196) was isolated via PCR from the following primers (5’-atgcgcatgctagtagggtggaggaagatg-3’ and 5’-gatcggatccttggtttaacactctaaagc-3’) and cloned into the SphI/BamHI restriction site of the pSPeCFP vector. To generate pSPDmrt.a construct, we isolated the coding sequence of *Dmrt.a* (Ciinte.CG.KH.S544.3) with following primers (5’-atgcgcggccgcatggcaaccgacagagga-3’ and 5’-gatcgaattcctacttgtcacttgagcatg-3’ and cloned into the NotI/EcoRI restriction site of pSPeCFP vector. To generate *Dmrt.a Δ MO target sequence>Dmr.a*, *Dmrt.a Δ MO target sequence* was inserted into the SphI and BamHI site of pSPDmrt.a construct. To generate the pSPMsxb MO target sequence CFP, *Msxb MO target sequence* (AAATTAAAAATGACAGTAAACGAAT) was tagged by inverse PCR. To generate *Msxb>Msxb MO target sequence CFP*, the enhancer sequence of *Msxb* was cloned into the XhoI/NotI site of the pSPMsxb MO target sequence CFP. To generate the pSPMsxb construct, we isolated the coding sequence of *Ci-Msxb* (Ciinte.CG.KH.C2.957) with the following primers (5’-atgcgcggccgcatgacagtaaacgaatcc-3’ and 5’-gcttgatatcctatcgactctcagttgggt-3’). To generate the pSPMsxb mut construct, we replaced the coding region of the *Msxb MO target sequence* from (ATGACAGTAACGAAT) to (ATGACGGTGAATGAGT) by inversePCR. The PCR products were digested with NotI and EcoRV and inserted into the NotI and blunted EcoRI sites of pSPeCFP. For *Msxb>Msxb mut*, the *Msxb* enhancer DNA was cloned into the XhoI/NotI site of pSPMsxb mut. To generate the pSPFoxc MO target sequence CFP, *Foxc* MO target sequence (GGTTTGATTCTCTATAATGACAATG) was tagged by inverse PCR. To generate *Foxc>Foxc MO target sequence CFP*, the enhancer sequence of *Foxc* was cloned into the XhoI/NotI site of pSPFoxc MO target sequence CFP. To generate the pSPFoxc construct, we isolated the coding sequence of *Ci-Foxc* (Ciinte.CG.KH.L57.25) with the following primers (5’-atgcgcggccgctatgacaatgcaaatccg-3’ and 5’-gatcgaattctcagtacttagtgtaatcgt-3’). To generate *Foxc>Foxc,* the enhancer sequence of *Foxc* was cloned into the XhoI/NotI site of pSPFoxc.

The following fusion genes were used for the experiments shown in Figure 2, Figure 3, and Extended Data Figure 3, Extended Data figure 4-The pSPDmrt.a, pSPSix1/2 and pSPFoxc fusion genes were prepared using the coding sequence of *Ci-Dmrt.a* (Ciinte.CG.KH.S544.3), *Ci-Six1/2* (Ciinte.CG.KH.C3.553) and *Ci-Foxc* (Ciinte.CG.KH.L57.25). These were amplified with the following primers (5’-atgcgcggccgcatggcagccaccctggcg-3’ and 5’-gatcgaattcttacgatcccatttcgactg-3’ for *Six 1/2*, 5’-atgcgcggccgctatgacaatgcaaatccg-3’ and 5’-gatcgaattctcagtacttagtgtaatcgt-3’ for *Foxc*). The PCR products were digested with NotI and EcoRI and inserted into the NotI and EcoRI site of pSPeCFP. To generate *Dmrt.a>Msxb*, *Dmrt.a>Six1/2* fusion genes, the enhancer region of *Dmrt.a* was inserted into the SphI and BamHI sites of pSPMsxb and pSPSix1/2. The *Dmrt.a>Foxc* fusion gene was prepared using the enhancer region of *Dmrt.a* inserted in the SphI and NotI sites of pSPFoxc. To generate, *Pax3/7>Foxc*, the enhancer region of *Pax3/7* was inserted into the XhoI and NotI sites of pSPFoxc. The minimal enhancer of *Six1/2* was amplified with the following primers (5’-tgcctgcagcgaaaacaatggtttatccg −3’ and 5’-gatcggatcctacatgtacgcgcactttaa-3’) and cloned into

the PstI/BamHI restriction site of a reporter construct containing the pSPFoxAa basal promoter and Kaede[33].

Microinjection of Antisense Morpholino Oligonucleotides and reporter genes.—Morpholino oligomers (MOs) were obtained from Gene Tools, LLC (Philomath, OR). MOs targeting *Dmrt.a, Msxb*, *Otx* and *Foxc* were described previously[15]. The following MO sequences were used: *Dmrt.a,* 5'-ctgtttgctataatttctgtaactc-3'; *Msxb,* 5'-attcgtttactgtcatttttaattt-3'; *Otx*, 5'-tacgacatgttaggaattgaacccg-3'. *Foxc* 5'-cattgtcattatagagaatcaaacc-3'. For control injections we used a universal control MO obtained from Gene Tools, LLC (Philomath, OR). MOs were dissolved in DEPC treated water containing 1mg/ml tetramethylrhodamine dextran (D1817, Invitrogen). The concentrations of MO and plasmid DNA in the injection medium were 0.5mM, 1–10ng/μl, respectively. Microinjections of MOs and reporter constructs were performed as described previously[34]. All experiments were repeated at least twice with different batches of embryos. Efficiency and specificity of MOs were evaluated by the simultaneous injection of MO and CFP reporter genes (10ng/μl), whereby the initiating codon (ATG) was replaced with a nucleotide sequence recognized by individual MOs (Extended Data Fig. 9). The concentration of rescue construct in the injection medium is 1ng/μl.

DiI labeling.—DiI or DiO labeling of the a5.3, a5.4, b5.3 blastomeres was performed as described previously[35,36]. DiI (Celltracker™ CM-DiI Dye, C7000, Molecular probe, Eugene, OR) and DiO (D-275, Molecular probe, Eugene, OR) were dissolved in soybean oil at a concentration of 5mg/ml. (see Extended Data Fig.1).

Single cell RNA-seq assays.—*Pax3/7>Foxc* (2.5ng/μl) injected eggs and control eggs were fertilized side by side, and allowed to develop to the late tailbud stage (12h after fertilization at 18°C). For each sample, 120 morphologically normal embryos were transferred into a 1.5 ml centrifuge tube that was pre-coated with 5% BSA in Ca^{2+}-Free artificial sea water (Ca^{2+}-Free ASW, 10 mM KCl, 40 mM $MgCl_2$, 15 mM $MgSO_4$, 435 mM NaCl, 2.5 mM $NaHCO_3$, 7 mM Tris base, 13 mM Tris-HCl). Cells were subsequently dissociated with 300 ul 1% trypsin in Ca^{2+}-Free ASW with 5 mM EGTA for 5 min. Embryos were pipetted 5 min on ice to complete dissociation of individual cells. 500 ul ice cold Ca^{2+}-Free ASW + 0.5% BSA was added to terminate digestion. Cells were collected by centrifuging at 900g for 5 min at 4°C and then resuspended in 50 ul ice cold Ca^{2+}-Free ASW + 0.5% BSA.

Single cell suspensions were loaded onto the 10x Genomics Chromium system using Reagent Kits to generate and amplify cDNAs, as recommended by the manufacturer (10X Genomics, CA)[37]. Illumina sequencing libraries were generated from the cDNA samples using the Nextera DNA library prep kit and sequenced using Illumina HiSeq 2500 Rapid flowcells (Illumina Inc., CA) with paired-end 26nt + 125nt reads following standard Illumina protocols. Raw sequencing reads were filtered by Illumina HiSeq Control Software and only Pass-Filter (PF) reads were used for further analysis.

The *Pax3/7>Foxc* and wildtype samples were run on a both lanes of a HiSeq 2500 Rapid Run mode flowcell. Basecalling was performed by Illumina RTA version 1.18.64.0. BCL

files were then converted to fastq format using Illumina's bcl2fastq version 1.8.4. Reads that aligned to phix (using Bowtie 1.1.1) were removed as well as reads that failed Illumina's default chastity filter. We then combined the fastq files from each lane and separated the samples using the barcode sequences allowing 1 mismatch (using barcode_splitter version 0.18.2). Using 10x CellRanger version 2.0.1, the count pipeline was run with default settings on the fastq files to generate gene-barcode matrices for each sample. The reference sequence was obtained from the Ghost database[38] with the *sv40* sequences added. The gene annotations used were also obtained from the Ghost database, again with *sv40* added.

Low-quality transcriptomes were filtered, as follows: 1) we discarded cells with less than 200 expressed genes; 2) we discarded cells with less than 500 or more than 30000 Unique Molecular Identifiers (UMIs). We further normalized the read counts of each cell by Seurat methods, and the normalized read counts were log-transformed for downstream analyses and visualizations. For dimensional reduction, the relative expression measurement of each gene was used to remove unwanted variation. Genes with the top 2000 highest standard deviations were obtained as highly variable genes of wild-type and transgenic (*Pax3/7>Foxc*) samples, respectively. We further aligned these two samples used canonical correlation analysis to focus on shared similarities and to facilitate comparative analysis. In aligned dataset, 10135 cells were kept and clustered based on their PCA scores with highly variable genes. Basically, after significant PCs were identified, a graph-based clustering approach was used for partitioning the cellular distance matrix into clusters. Cell distance was visualized by t-Distributed Stochastic Neighbor Embedding (t-SNE) method in reduced 2D space. Differentially expressed genes (DEGs) between different cell types were identified by the following criteria using the DESeq2 software package: 1) FDR adjusted p value < 0.01; 2) absolute log2 fold change between groups were larger than 1.

Extended Data

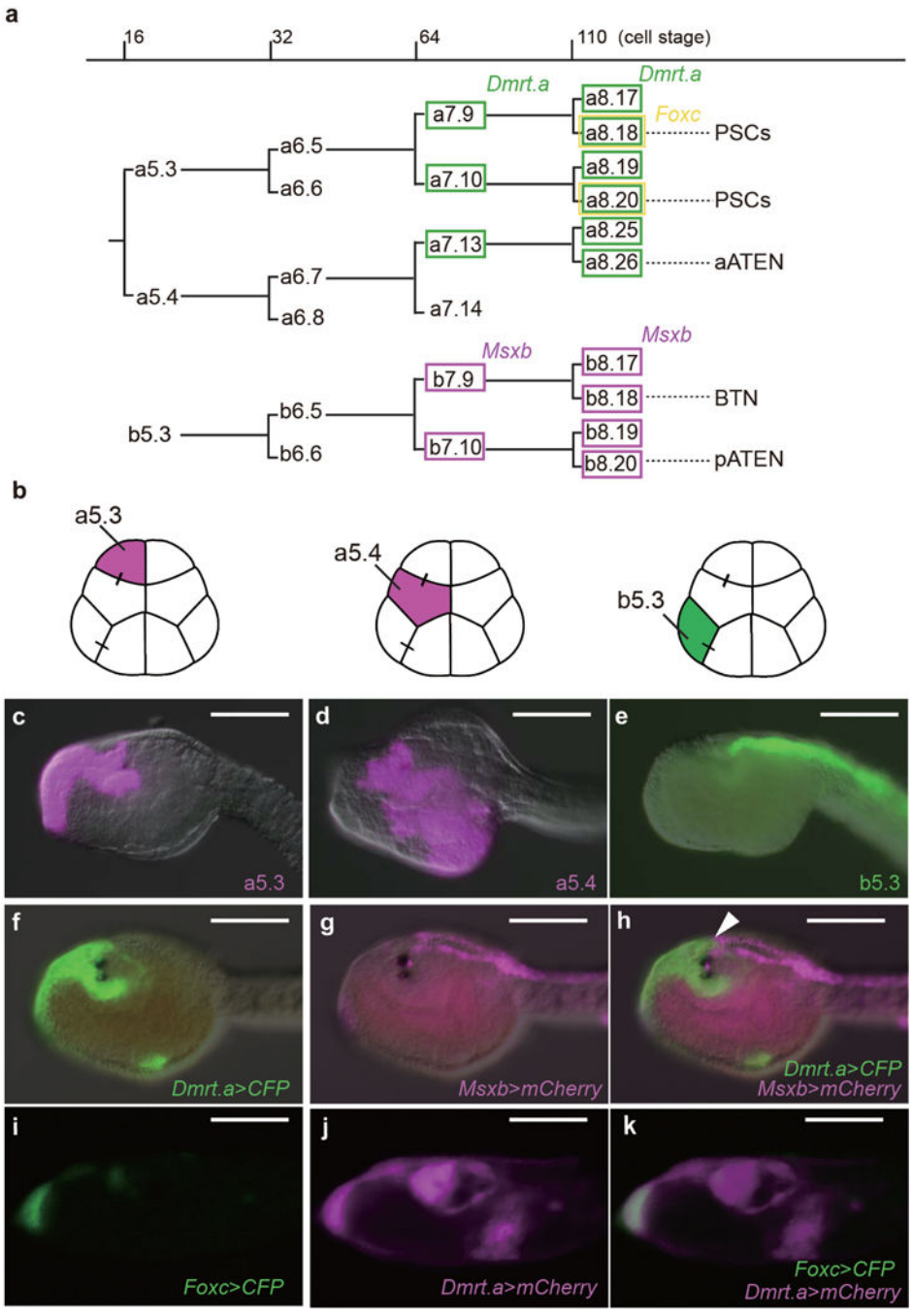

Extended Data Figure 1. Sensory cell lineages.

a, Cell lineages of anterior blastomeres (a-line blastomeres) and a posterior blastomere (b-line) from the 16-cell to 110-cell stages. Green identifies *Dmrt.a*-expressing blastomeres, magenta identifies *Msxb* expression lineages, and yellow identifies *Foxc* expression. **b,** Schematic illustration of 16 cell stage embryos. Each of the blastomeres that was labeled with Dil or DiO is indicated by magenta or green. **c-e**, Head regions of larvae labeled with

DiI or DiO at the 16 cell stage. **c**, Labeling of the a5.3 lineage. **d**, Labeling of the a5.4 lineage. **e,** labeling b5.3 blastomere. **f-h**, Head region of a larva that was co-injected with *Dmrt.a>CFP* and *Msxb>mCherry* reporter genes. Arrowhead identifies the boundary of the *Dmrt.a/Msxb* expression territories. **i-k,** Head region of a larva co-injected with *Foxc>CFP* and *Dmrt.a>mCherry* reporter genes. Anterior to the left; scale bars, 100μm.

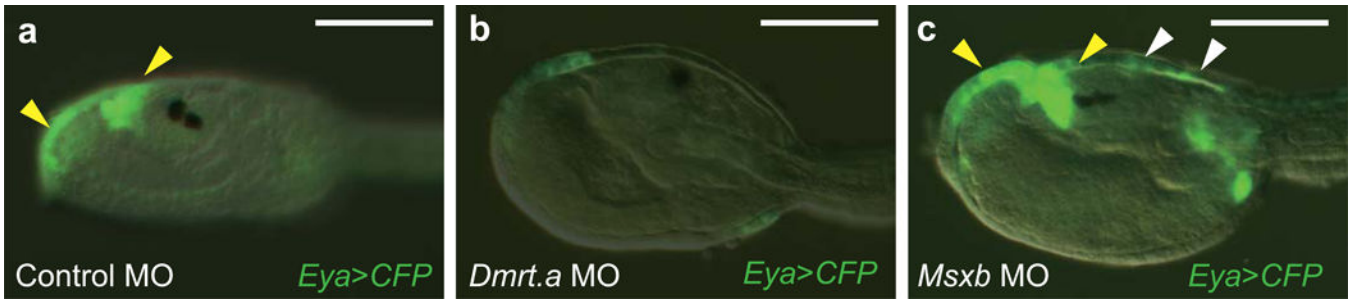

Extended Data Figure 2. Regulation of *Eya* expression by *Dmrt.a* and *Msxb*.

a-c, Head regions of larvae injected with an *Eya>CFP* reporter gene. Yellow arrowheads denote *Eya* expression in the proto-placodal region of Control MO injected larvae (36 of 36 larvae displayed this pattern) (**a**). **c**, there is expanded expression (white arrowheads) in *Msxb* morphants (39 of 48 larvae showed this phenotype). **b**, there is a loss of expression in *Dmrt.a* morphants (88 of 88 larvae showed this phenotype). Anterior to the left; scale bars, 100μm.

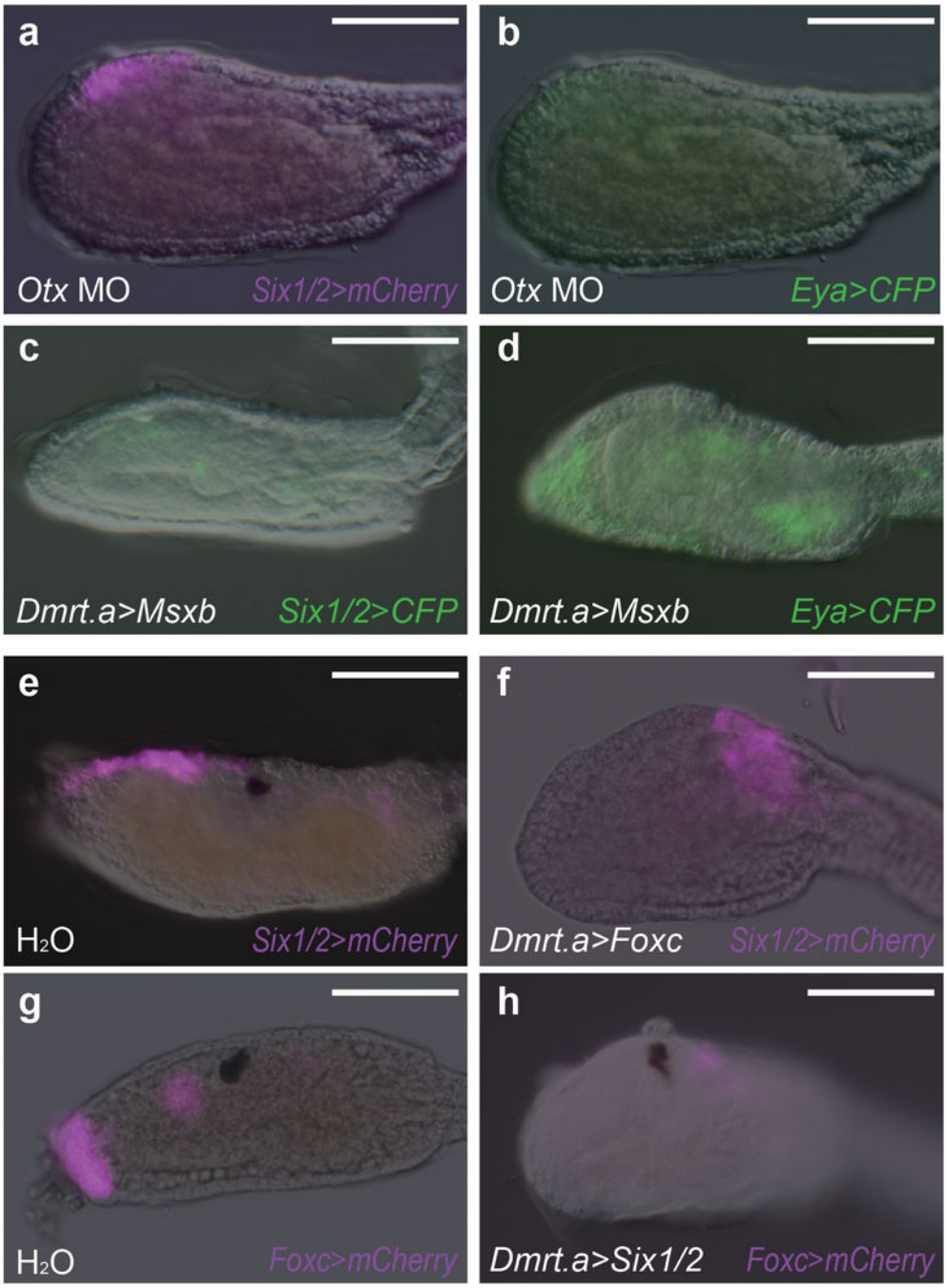

Extended Data Figure 3. Regulatory interactions among placodal determinants.

a, b, Head regions of larvae that were injected with an *Otx* MO, and co-injected with *Six1/2>mCherry* (**a**) and *Eya>CFP* (**b**) (32 of 32 larvae showed reduced or no expression of *Six1/2>mCherry* and no expression of *Eya>CFP*). **c**, **d**, Head regions of larvae injected with *Dmrt.a>Msxb*, and co-injected with *Six1/2>CFP* (33 of 33 larvae showed no expression of *Six1/2>CFP*) (**c**) and *Eya>CFP* (71 of 71 larvae showed little or no expression of *Eya>CFP*) (**d**). **e**, **f**, Head regions of larvae injected with *Six1/2>mCherry*, and co-injected with H_2O (61 of 61 larvae showed full expression of *Six1/2>mCherry*) (**e**), or *Dmrt.a>Foxc* (50 of 50

larvae showed no expression of *Six1/2>mCherry*) (**f**). **g**, **h**, Head regions of larvae injected with *Foxc>mCherry,* and co-injected with H_2O (40 of 40 larvae showed full expression of *Foxc>mCherry* (**g**) or *Dmrt.a>Six1/2* (39 of 39 larvae showed no expression of *Foxc>mCherry*) (**h**). Scale bars, 100μm.

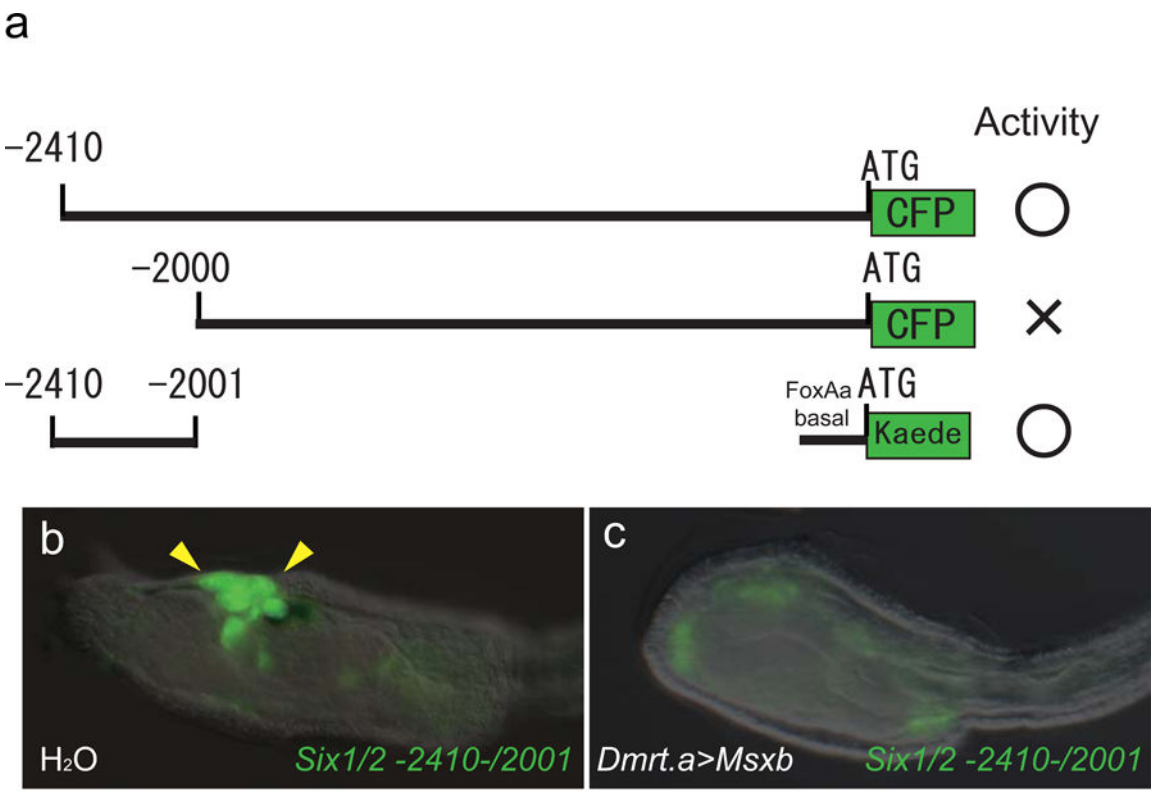

d

-2410 CGAAAACAATGGTTTATCCGAGGTAGTAGAGTAGATTTCTGAGCAACACA
GAAAGTTTGTAACAACAATGAAAGAATATTAAACGCACTGAGATTATTGT
-2310 AATTGTAGTAATATAGCTTTCACATTTTCAAACGATCTGTCAACTGCTAA
ACTGCCAATTAATATTAACGCATATTTGCATAGCAATTATTTACTAATTC
-2210 CGACACGCAAGGACCGATTTCCCAACTCTGTTTGATCAAAGGGAATCGCT
TTGCTTGTTTAATGCGATCATCAACGCTACAAATGTCAGCAATCGGATAT
-2110 TTTAAGCTCCGTATTAAGTCACGTGCTACGAGCGTGATGAAGTGGAACGA
GTTGTTTACTTTTAAACTCACGTGGCGTTAATTGGTCGGATTAAAGTGCG
-2010 CGTACATGTA

Extended Data Figure 4. Direct repression of *Six1/2* expression by *Msxb*.

a Deletion analyses of the 5' regulatory region of *Six1/2*. −2410 bp to −2001 bp of the 5' *cis*-regulatory region is necessary for *Kaede* expression in the pre-placodal territory. **b, c,**

head regions of larvae injected with *Six1/2 −2410/−2001>Kaede*, and co-injected with H_2O (74 of 74 larvae showed full expression of *Six1/2 −2410/−2001>Kaede*) or *Dmrt.a>Msxb* (37 of 37 larvae showed no expression of *Six1/2 2410/−2001>Kaede*) (**c**). **d**, the *Six1/2* 5' regulatory region spanning −2410 to −2001 bp contains an *Otx* binding site (green box) and multiple *Msxb* repressor binding sites (magenta box).

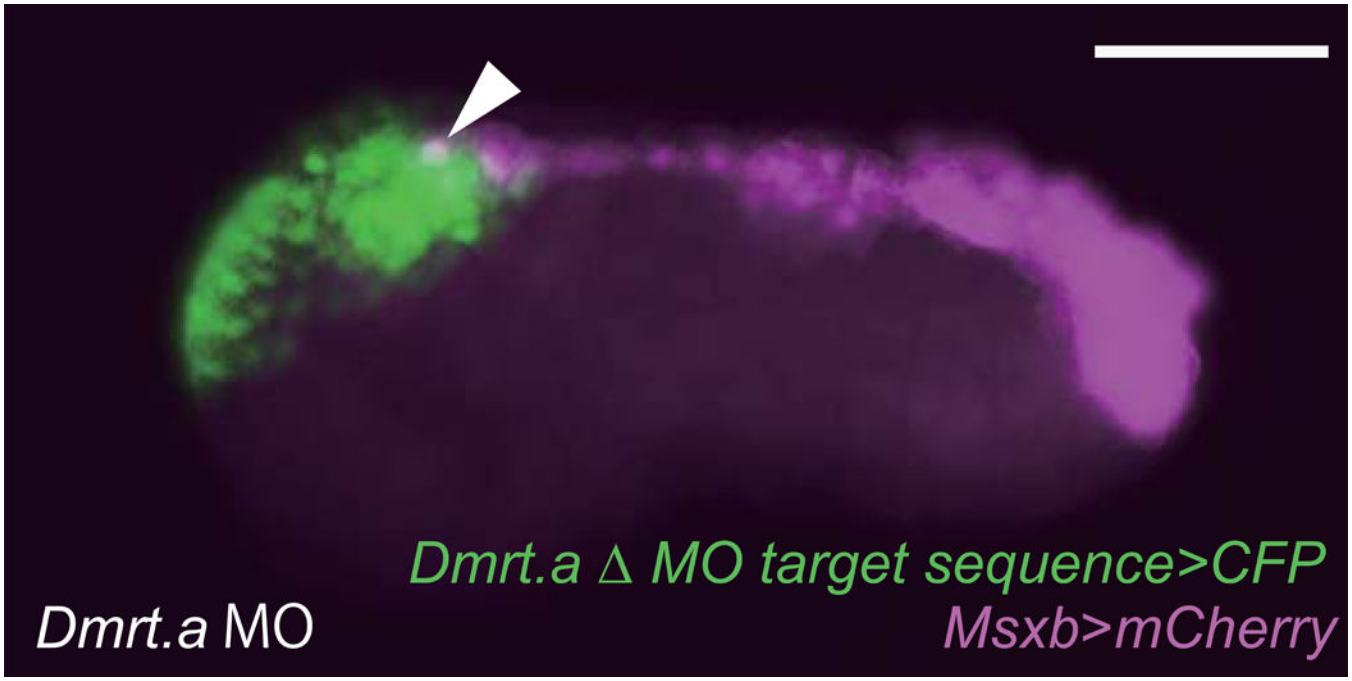

Extended Data Figure 5. Anterior expansion of *Msxb* expression in *Dmrt.a* morphant.
Tailbud embryo co-injected with *Dmrt.a* MO, *Dmrt.a Δ MO target sequence>CFP* and *Msxb>mCherry* construct. The anterior expansion of the *Msxb>mCherry* expression pattern is indicated by the white arrowhead. Anterior to the left; scale bars, 100μm

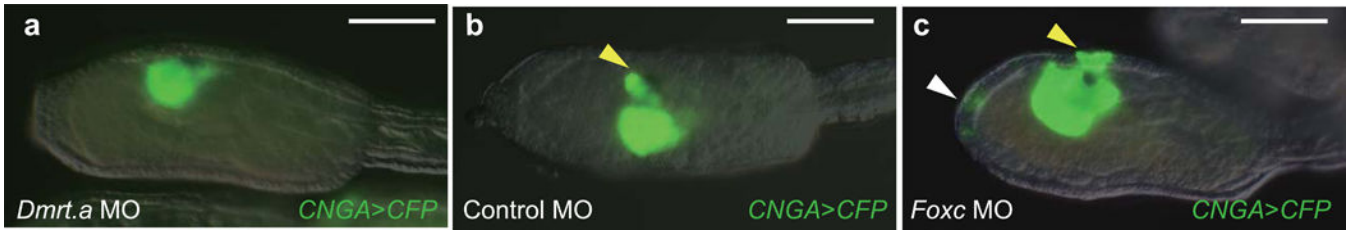

Extended Data Figure 6. Specification of aATEN sensory neurons.
a-c, Larvae injected with *CNGA>CFP* reporter gene. Yellow arrowheads indicate expression in aATENs, and white arrowheads indicate ectopic sites of differentiated aATENs in the palp. **a,** Larva co-injected with *Dmrt.a* MO (62 of 62 larvae showed no expression of *CNGA>CFP* in aATENs). **b,** Larva co-injected with control MO (32 of 32 larvae showed full expression of *CNGA>CFP*). **c,** Larva co-injected with *Foxc* MO (18 of 42 larvae showed expanded expression of *CNGA>CFP* in palp region). Anterior to the left; scale bars, 100μm.

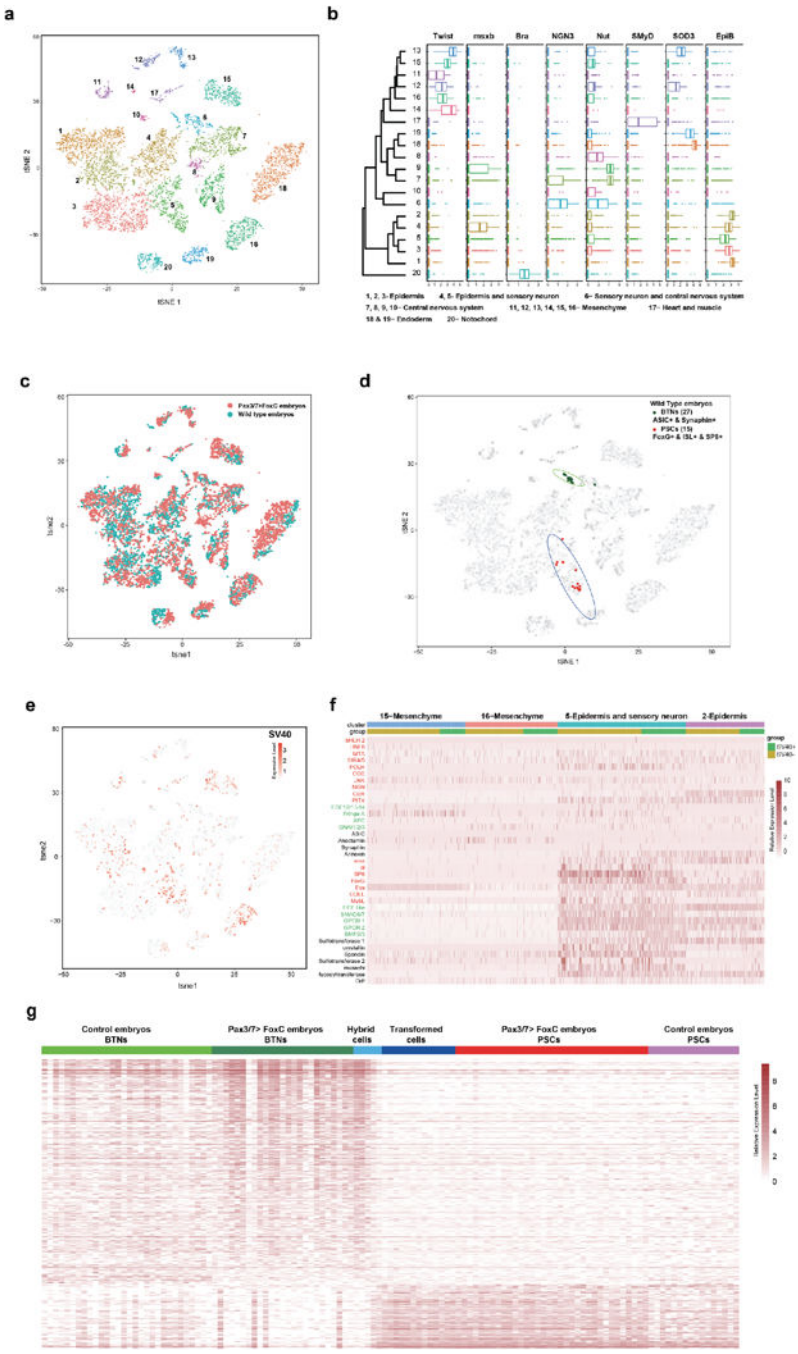

Extended Data Figure 7. Single Cell RNA-seq analysis. .

a, **b,** Identification of major cell types among 20 clusters with known markers, 3 epidermis clusters were identified by the expression of *EpiB*; 2 clusters of epidermis and sensory neurons were identified by the expression of either *Msxb* or *Nut,* along with *EpiB*; a cluster of sensory neurons identified by the expression of *NGN3* and *Nut*; 3 clusters of central nervous system by high levels of *Nut* transcripts; 6 clusters of mesenchyme by their expression of *Twist*; 2 endoderm clusters by the high expression of *SOD3*; and one notochord cluster by the expression of *Ci-T* (*Brachyury*). **c,** Representation of overlap

between cells from *Pax3/7>Foxc* and control embryos in each cell population. tSNE plot from Figure 3a, with each cell now colored to indicate their origin from either *Pax3/7>Foxc* embryos (red dots, n=5339) or control embryos (blue dots, n=4850). Both samples contribute to all 20 cell populations. d, Identification of BTNs and PSCs with the combination of representation markers in the control embryo, 27 BTNs (green dot) were identified by the combination of *Asic1b* & *Synaphin*, and 15 PSCs were identified by the combination of *Foxg*, *islet*, and *SP8*. **e,** Visualization of SV40 positive cells in *Pax3/7>Foxc* transgenic embryos within tSNE projection map. SV40 is detected in cells contained within clusters 2 and 5 for epidermis and sensory neuron cells, as well as weak expression in mesenchyme clusters 15 and 16. None of the transformed or hybrid cells contained in the sensory cell clusters (5 and 6) express any mesenchyme marker genes, suggesting that none of these are transformed by misexpression of *Pax3/7*. **f,** heatmap of representative genes (see Fig. 3e of main text) that show no significant differential expression in SV40 positive cells contained within clusters 2, 5, 15, and 16. **g,** heatmap of all differentially expressed genes between BTNs and PSCs from both control and *Pax3/7>Foxc* embryos.

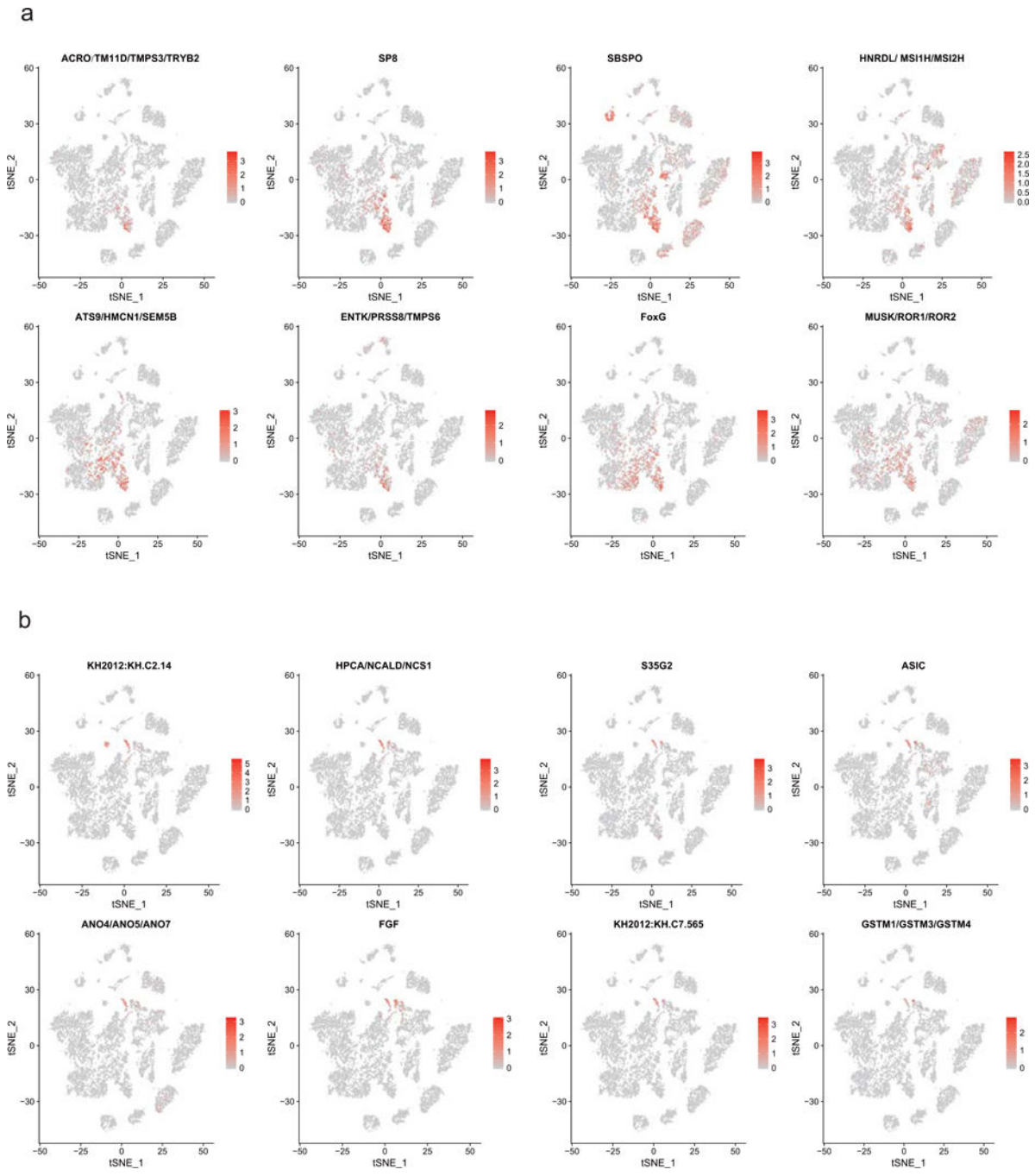

Extended Data Figure 8. New identified markers for PSCs and BTNs.
Distribution of new identified marker gene in PSCs (a) and BTNs (b).

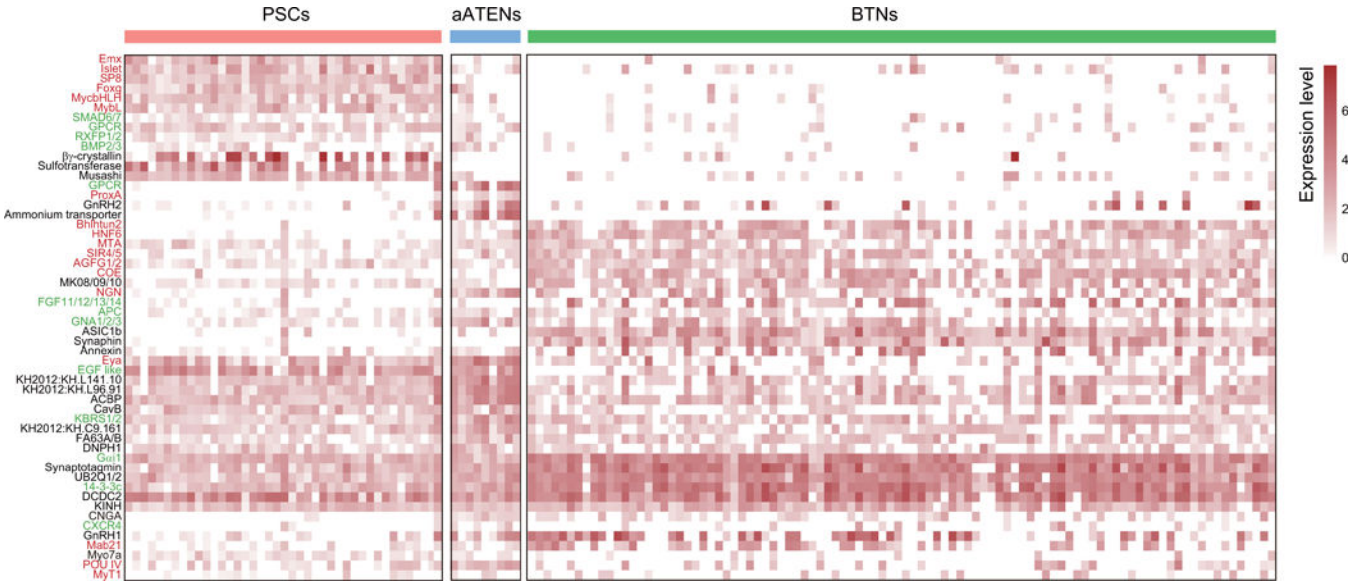

Extended Data Figure 9. Heatmap of differentially expressed and co-expressed genes between PSCs, aATENs and BTNs from rom wild type late tailbud stage II embryos.

Transcription factors (red), signaling pathway genes (green), and effector genes (black).

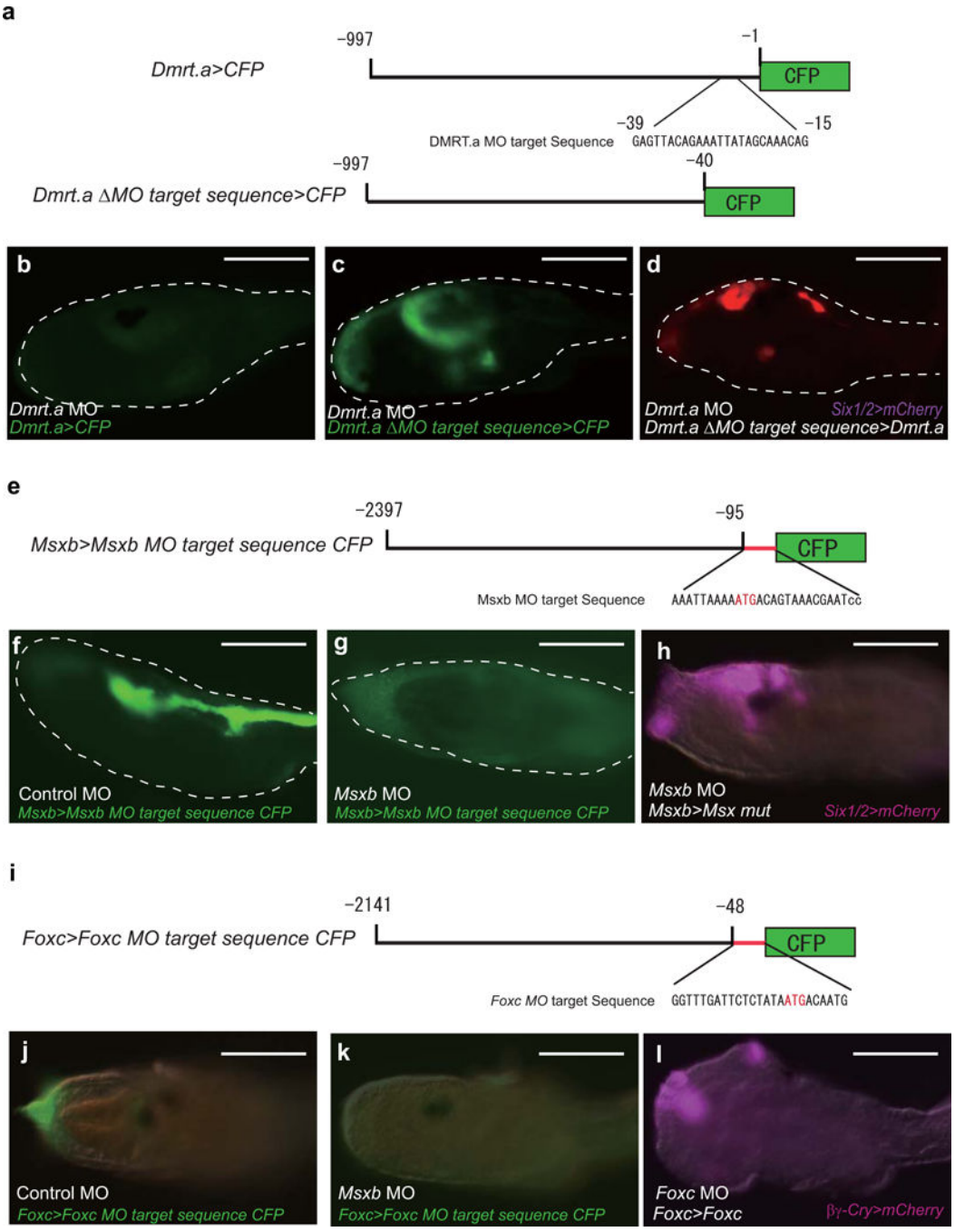

Extended Data Figure 10. Control experiments for MO gene disruption assays.

a-d, *Dmrt.a* MO. **a,** Schematic diagram of reporter gene containing *Dmrt.a* regulatory genes with and without recognition sequences for the *Dmrt.a* MO that was used in this study. The MO recognition sequences are located in the 5' UTR, upstream of the initiating AUG codon (−1). **b,** Larva injected with *Dmrt.a* MO and co-injected with the *Dmrt.a>CFP* reporter gene containing the MO recognition sequences. 46 of 46 larvae showed no protein synthesis from the *Dmrt.a>CFP* reporter. **c**, Same as **b** except that the reporter gene lacks the *Dmrt.a* MO recognition sequence (*Dmrt.a ΔMO target>CFP*). 57 of 57 larvae showed C*FP* expression in

appropriate head tissues. *Dmrt.a* MO efficiently blocks the expression of *CFP* that contains the *Dmrt.a MO* target sequence. **d,** Larva co-injected with *Dmrt.a* MO*, Dmrt.a ΔMO>Dmrt.a* and *Six1/2>mCherry. Dmrt.a* MO morphants normally lack *Six1/2>mCherry* expression (see Fig. 2b), but expression is restored with a *Dmrt.a* transgene that lacks the MO recognition sequence (107 of 108 larvae showed expression of *Six1/2>mCherry*). This result shows that the *Dmrt.a* MO used in this study specifically blocks the synthesis of *Dmrt.a* protein products. **e-h,** *Msxb* MO. **e,** Diagram of *Msxb* 5' regulatory region and the location of the recognition sequences for the *Msxb* MO and point mutations in this sequence. **f, g**, Larvae injected with *Msxb> CFP* containing MO recognition sequences, and co-injected with control MO (54/54 larvae showed CFP expression) (**f**). **g**, Same as **f** except that the *Msxb* MO was coinjected in place of the control MO (44/44 larvae showed no expression of CFP). These results show that the *Msxb* MO specifically blocks *CFP* protein synthesis from the *Msxb* reporter gene. **h**, Larva co-injected with *Msxb* MO, *Six1/2>mCherry*, and *Msxb>CFP* reporter gene containing point mutations in MO recognition sequence (see red letters in panel **e**). *Msxb* morphants normally display expanded expression of *Six1/2* in tail regions (see Figure 2c). This expansion is suppressed by co-injection of the mutant *Msxb* transgene lacking MO recognition sequences (**h**). This result suggests that the *Msxb* MO inhibits synthesis of Msxb protein products. **i-l**, *Foxc* MO. **i**, Diagram of *Foxc 5'* regulatory region showing the location of the MO recognition sequence and point mutations in this sequence. **j-l**, Larvae injected with *Foxc>Foxc* transgene and *Foxc>CFP* reporter gene, and also co-injected with control MO (25/25 larvae showed *CFP* expression) (**j**). **k**, Same as **j** except that the embryo was co-injected with the *Foxc* MO in place of the control MO (99/99 larvae showed no expression of CFP) (**k**). This result shows that the *Foxc* MO efficiently blocks the synthesis of CFP proteins encoded by the *Foxc>CFP* reporter gene containing the *Foxc MO target sequence*. **l**, Larvae co-injected with *Foxc* MO, *Foxc>Foxc mut* (MO-resistant *Foxc* cDNA) and *βγ-crystallin>mCherry.* Normally, *Foxc* morphants lack expression of the *βγ-crystallin>mCherry* reporter gene (see Figure 2f). However, expression is restored by co-injection of *Foxc>Foxc* transgene. This result suggests that the *Foxc* MO inhibits synthesis of Foxc protein products. Scale bar, 100μm.

Supplementary Material

Refer to Web version on PubMed Central for supplementary material.

Acknowledgments

We thank all the members of the LSI genome facility for technical support of the single cell RNA-seq assays and analysis. We also thank Reiko Yoshida and Chikako Imaizumi and all other members of the staff at the Maizuru Fisheries Research Station of Kyoto University for providing *Ciona intestinalis*. This study was supported by a grant from the NIH to M.L. (NS076542) and by Grants-in-Aid for Scientific Research from JSPS to T.H. (24687008, 16K07433). T.H. was supported by the Pre-Stagic Initiatives, University of Tsukuba. Portion of *Ciona intestinalis* and plasmids used in this study were provided by the National Bio-Resource Project (NBRP) of the MEXT, Japan. A. H. was partially supported by a fellowship from the Colombian Government (Colciencias 568).

REFERENCE

1. Northcutt RG & Gans C The genesis of neural crest and epidermal placodes: a reinterpretation of vertebrate origins. Q. Rev. Biol 58, 1–28 (1983). [PubMed: 6346380]

2. Baker CV & Bronner-Fraser M The origins of the neural crest. Part II: an evolutionary perspective. Mech. Dev 69, 13–29 (1997). [PubMed: 9486528]
3. Schlosser G Do vertebrate neural crest and cranial placodes have a common evolutionary origin? Bioessays 30, 659–672 (2008). [PubMed: 18536035]
4. Schlosser G, Patthey C & Shimeld SM The evolutionary history of vertebrate cranial placodes II. Evolution of ectodermal patterning. Dev. Biol 389, 98–119 (2014). [PubMed: 24491817]
5. Stolfi A et al. Migratory neuronal progenitors arise from the neural plate borders in tunicates. Nature 527, 371–374 (2015). [PubMed: 26524532]
6. Wagner E et al. Islet is a key determinant of ascidian palp morphogenesis. Development 141, 3084–3092 (2014). [PubMed: 24993943]
7. Manni L et al. Neurogenic and non-neurogenic placodes in ascidians. J. Exp. Zool. B Mol. Dev. Evol 302, 483–504 (2004). [PubMed: 15384166]
8. Mazet F et al. Molecular evidence from Ciona intestinalis for the evolutionary origin of vertebrate sensory placodes. Dev. Biol 282, 494–508 (2005). [PubMed: 15950613]
9. Pasini A et al. Formation of the ascidian epidermal sensory neurons: insights into the origin of the chordate peripheral nervous system. PLoS Biol 4, e225 (2006). [PubMed: 16787106]
10. Imai JH & Meinerzhagen IA Neurons of the ascidian larval nervous system in Ciona intestinalis: II. Peripheral nervous system. J. Comp. Neurol 501, 335–352 (2007). [PubMed: 17245709]
11. Horie T, Kusakabe T & Tsuda M Glutamatergic networks in the Ciona intestinalis larva. J. Comp. Neurol 508, 249–263 (2008). [PubMed: 18314906]
12. Wagner E & Levine M FGF signaling establishes the anterior border of the Ciona neural tube. Development 139, 2351–2359 (2012). [PubMed: 22627287]
13. Patthey C, Schlosser G & Shimeld SM The evolutionary history of vertebrate cranial placodes--I: cell type evolution. Dev. Biol 389, 82–97 (2014). [PubMed: 24495912]
14. Abitua PB et al. The pre-vertebrate origins of neurogenic placodes. Nature 524, 462–465 (2015). [PubMed: 26258298]
15. Imai KS et al. Regulatory blueprint for a chordate embryo. Science 312, 1183–1187 (2006). [PubMed: 16728634]
16. Tresser J et al. doublesex/mab3 related-1 (dmrt1) is essential for development of anterior neural plate derivatives in Ciona. Development 137, 2197–2203 (2010). [PubMed: 20530547]
17. Aniello F et al. Identification and developmental expression of Ci-msxb: a novel homologue of Drosophila msh gene in Ciona intestinalis. Mech. Dev 88, 123–126 (1999). [PubMed: 10525197]
18. Wada H et al. Neural tube is partially dorsalized by overexpression of HrPax-37: the ascidian homologue of Pax-3 and Pax-7. Dev. Biol 187, 240–252 (1997). [PubMed: 9242421]
19. Huang X et al. The doublesex-related gene, XDmrt4, is required for neurogenesis in the olfactory system. Proc. Natl. Acad. Sci. U. S. A 102, 11349–11354 (2005). [PubMed: 16061812]
20. Parlier D et al. The Xenopus doublesex-related gene Dmrt5 is required for olfactory placode neurogenesis. Dev. Biol 373, 39–52 (2013)21.
21. Ahrens K & Schlosser G Tissues and signals involved in the induction of placodal Six1 expression in Xenopus laevis. Dev. Biol 288, 40–59 (2005). [PubMed: 16271713]
22. Schlosser G & Ahrens K Molecular anatomy of placode development in Xenopus laevis. Dev. Biol 271, 439–466 (2004). [PubMed: 15223346]
23. Pieper M et al. Origin and segregation of cranial placodes in Xenopus laevis. Dev. Biol 360, 257–275 (2011). [PubMed: 21989028]
24. Köster M et al. Activin A signaling directly activates Xenopus winged helix factors XFD-4/4', the orthologues to mammalian MFH-1. Dev. Genes Evol 210, 320–324 (2000). [PubMed: 11180837]
25. Bailey AP et al. Lens specification is the ground state of all sensory placodes, from which FGF promotes olfactory identity. Dev. Cell 11, 505–517 (2006). [PubMed: 17011490]
26. Berry FB et al., Functional interactions between FOXC1 and PITX2 underlie the sensitivity to FOXC1 gene dose in Axenfeld-Rieger syndrome and anterior segmentdysgenesis. Hum. Mol. Genet 15, 905–919 (2006). [PubMed: 16449236]

27. Corbo JC, Levine M & Zeller RW Characterization of a notochord-specific enhancer from the Brachyury promoter region of the ascidian, Ciona intestinalis. Development 124, 589–602 (1997). [PubMed: 9043074]

28. Schlosser G Induction and specification of cranial placodes. Dev. Biol 294, 303–351 (2006). [PubMed: 16677629]

29. Abitua PB et al., Identification of a rudimentary neural crest in a non-vertebrate chordate. Nature 492, 104–107. (2012). [PubMed: 23135395]

30. Gainous TB, Wagner E & Levine M Diverse ETS transcription factors mediate FGF signaling in the Ciona anterior neural plate. Dev. Biol 399, 218–225. (2015). [PubMed: 25576927]

31. Russo MT et al. Regulatory elements controlling Ci-msxb tissue-specific expression during Ciona intestinalis embryonic development. Dev. Biol 267, 517–528. (2004). [PubMed: 15013810]

32. Roure A, Lemaire P & Darras S An otx/nodal regulatory signature for posterior neural development in ascidians. PLoS Genet 10, e1004548 (2014). [PubMed: 25121599]

33. Hozumi A et al. Enhancer activity sensitive to the orientation of the gene it regulates in the chordate genome. Dev. Biol 375, 79–91 (2013). [PubMed: 23274690]

34. Satou Y, Imai KS & Satoh N Action of morpholinos in Ciona embryos. Genesis 30, 103–106. (2001). [PubMed: 11477683]

35. Satou Y, Imai KS & Satoh N The ascidian Mesp gene specifies heart precursor cells. Development 131, 2533–2541. (2004). [PubMed: 15115756]

36. Horie T et al. Ependymal cells of chordate larvae are stem-like cells that form the adult nervous system. Nature 469, 525–528. (2011). [PubMed: 21196932]

37. Zheng GX et al. Massively parallel digital transcriptional profiling of single cells. Nature communications, 8, p.14049 (2017).

38. Satou Y et al. An integrated database of the ascidian, Ciona intestinalis: towards functional genomics. Zoolog. Sci 22, 837–843. (2005). [PubMed: 16141696]

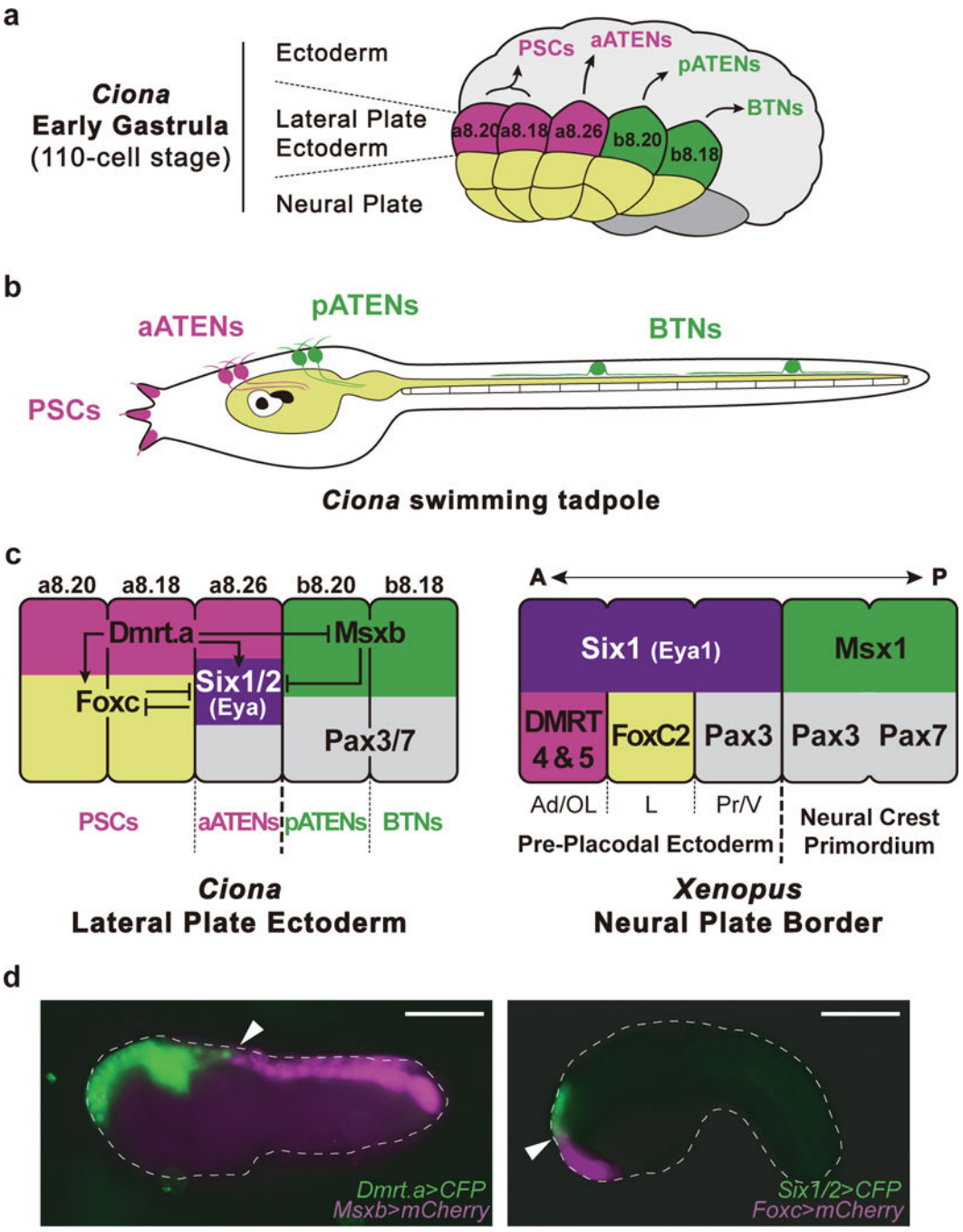

Figure 1 |. Lateral plate ectoderm.

a, Summary of lateral plate derivatives at early gastrula (110 cell stage). Magenta indicates progenitors of palp sensory cells (PSCs) and aATENs arising from the a8.20, a8.18 and a8.26 lineages, respectively. Green indicates pATENs and BTNs arising from b8.20 and b8.18, respectively. **b,** Diagram of *Ciona* tadpole showing the position of PSCs, aATENs, pATENs and BTNs. **c,** Summary of *Ciona* lateral plate ectoderm and *Xenopus* pan-placodal primordium. Magenta indicates *Dmrt.a* expressing blastomeres (a8.20, a8.18 and a8.26 lineage), green indicates *Msxb* expressing blastomeres (b8.20 and b8.18 lineage), violet

indicates prospective *Six1/2* and *Eya* expressing blastomeres (a8.26 lineage), yellow indicates *Foxc* expressing blastomeres (a8.20 and a8.18 lineage) and grey indicates *Pax3/7* expressing blastomeres (a8.26, b8.20 and b8.18 lineage), A, anterior; Ad, adenohypophyseal placode; OL, olfactory placode; L, lens placode; P, posterior; Pr, profundal placode; V, trigeminal placode. **d,** (left) Tailbud embryo co-injected with *Dmrt.a>CFP* (green) and *Msxb>mCherry* (magenta) reporter genes. Arrowhead indicates the boundary separating the *Dmrt.a* and *Msxb* expression territories. **d**, (right) Tailbud embryo injected with *Six1/2>CFP* and *Foxc>mCherry* reporter genes. Arrowhead indicates the boundary separating the *Six1/2* and *Foxc* expression territories. Anterior to the left; scale bars, 100 μm.

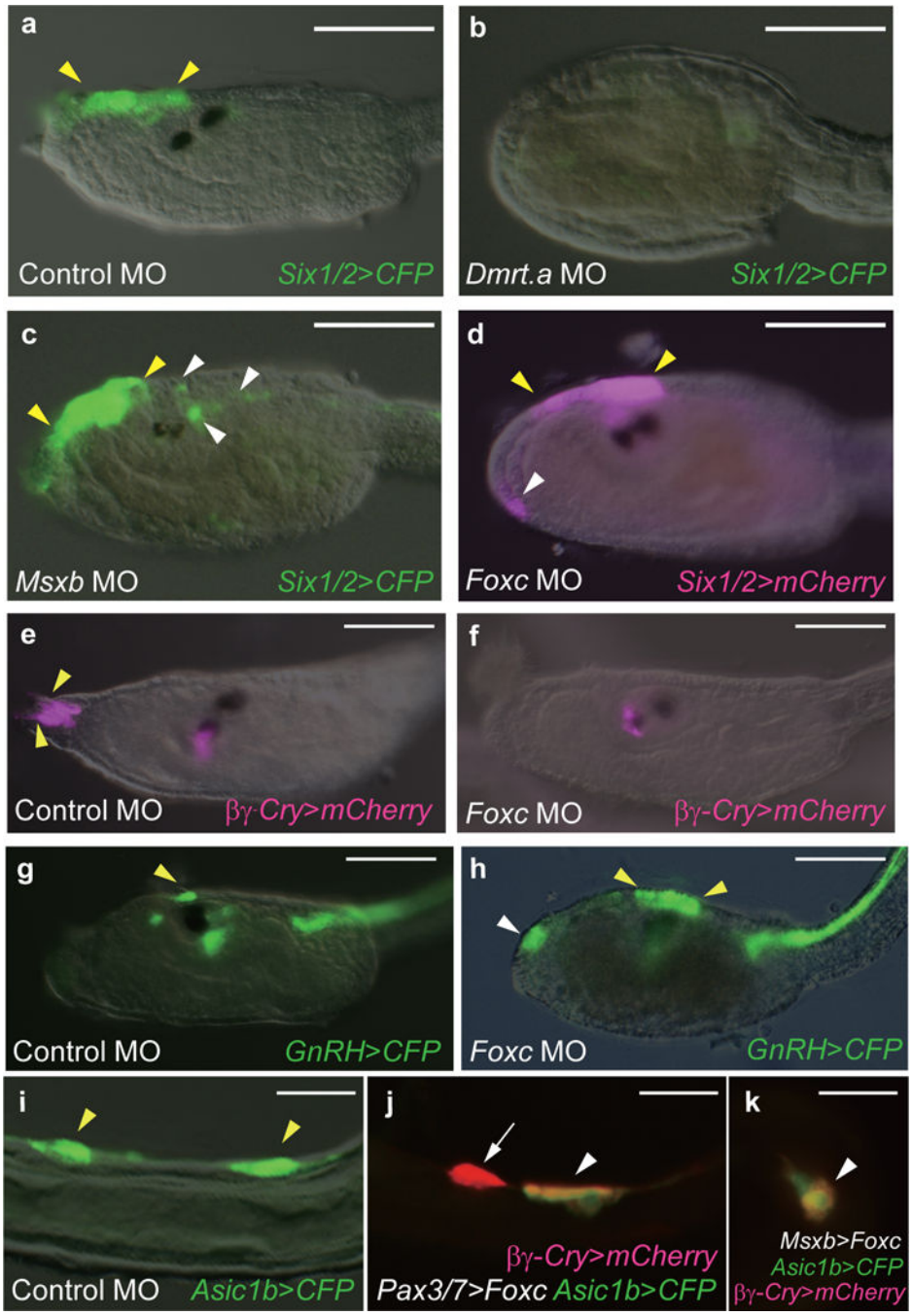

Figure 2 |. Functional analysis of the lateral plate ectoderm.

a-c, Head regions of larvae that were injected with a *Six1/2>CFP* reporter gene. **a**, *Six1/2* expression in the proto-placodal region of control MO injected tadpoles (49 of 49 larvae displayed this expression pattern). The yellow arrowheads identify the normal location of *Six1/2* expression. **b**, Loss of expression in *Dmrt.a* morphants (49 of 49 larvae). **c,** Expanded expression of the *Six1/2>CFP* reporter gene (white arrowheads) in *Msxb* morphants (42 of 50 larvae showed this expansion pattern). **d,** Head regions of a larva that was co-injected with *Foxc* MO and *Six1/2>mCherry* reporter gene. There is ectopic expression (white

arrowhead) in the palp regions of *Foxc* morphants (35 of 47 larvae showed this phenotype). **e, f,** Larvae injected with *βγ-crystallin>mCherry* reporter gene. Yellow arrowheads indicate the *βγ-crystallin* expressing PSCs in control MO injected larvae (51 of 51 larvae display this expression pattern). **f**, There is a loss of these cells in *Foxc* morphants (108 of 108 larvae showed this phenotype). **g, h,** Larvae injected with a *GnRH>CFP* reporter gene. Yellow arrowheads identify the *GnRH* expressing aATENs in a control larva (59 of 59 larvae displayed expression in aATENs). **h,** There is ectopic expression in the palp regions of *Foxc* morphants (white arrow) (28 of 40 injected larvae showed this phenotype). **i-k**, Tail regions of larvae injected with *Asic1b>CFP* (**i**) and co-injected with *βγ-crystallin>mCherry* reporter gene (**j**,**k**). Yellow arrowheads identify the *Asic1b* expressing BTNs in a control larva (83 of 83 larvae displayed this phenotype). **j,** Ectopic expression of the *βγ-crystallin>mCherry* reporter gene in tail regions (white arrowheads) upon misexpression of *Foxc* by the *Pax3/7* enhancer (26 of 55 larvae showed this phenotype. **k**, Same as **j** except that *Msxb* regulatory sequences were used to misexpress *Foxc* (31 of 57 larvae showed misexpression of *βγ-crystallin>mCherry*. Anterior to the left; scale bars, 100 μm (**a-h**), 20 μm (**i-k**).

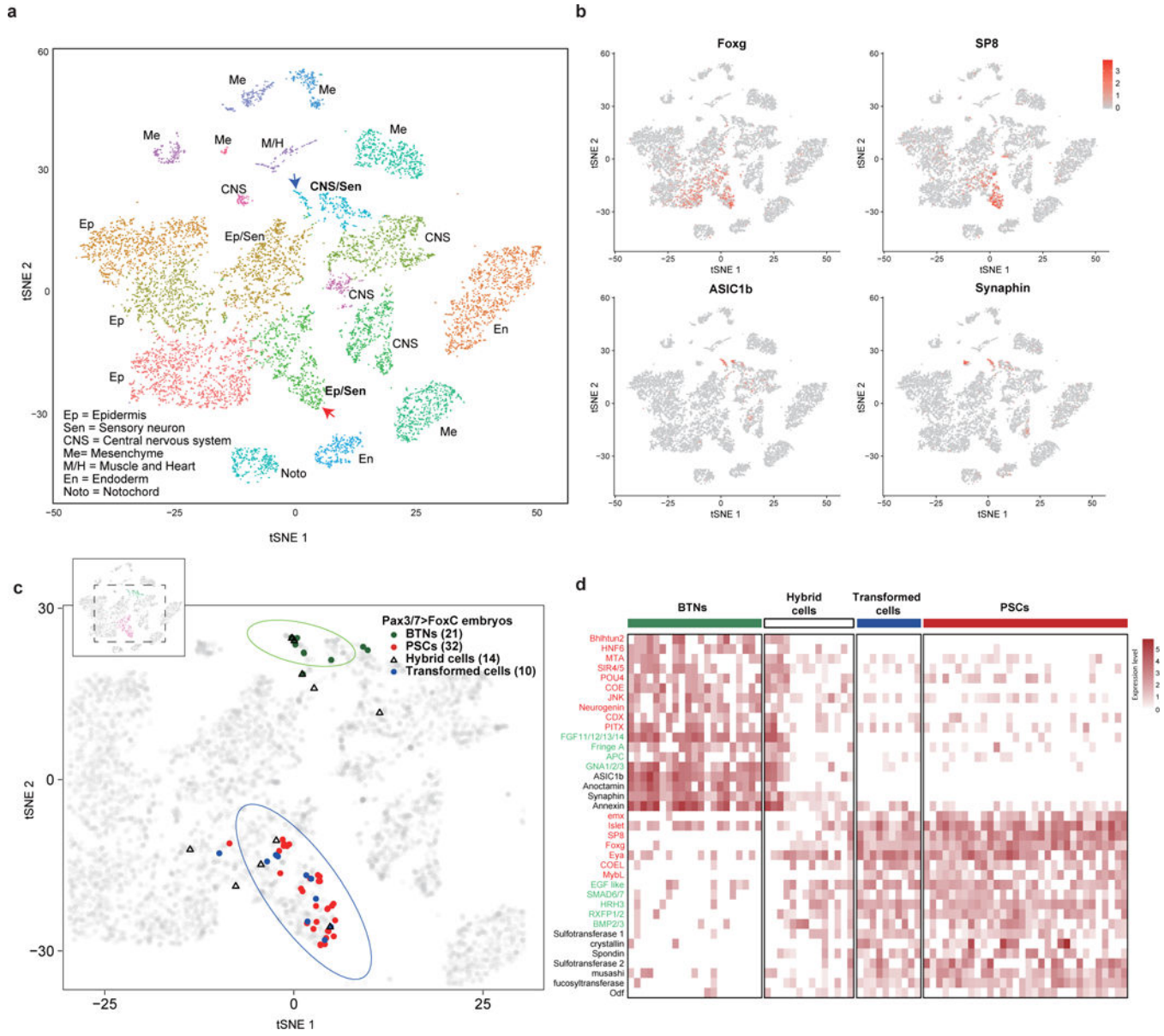

Figure 3 |. Single cell RNA-seq analysis of BTN transformations.

a, The tSNE projection map of dissociated cells from wild-type and mutant tailbud-stage embryos that misexpress *Foxc* in tail regions using *Pax3/7* regulatory DNAs (*Pax3/7>Foxc* transgene). Each dot corresponds to the transcriptome of a single cell, and cells possessing similar transcriptome profiles map near each other. All of the major tissue types in tailbud-stage embryos were identified: Ep=epidermis; Se=sensory neurons; CNS=central nervous system; Me=mesenchyme; M&H=heart and muscle; En=Endoderm; Noto=Notochord). Identification is based on the expression of known marker genes (Extended Data Fig. 8b, and Extended File 1 sheet 1). **b**, Distribution of marker gene expressed in PSCs (*Islet*, *Foxg* and *SP8*) and BTNs (*Asic1b* and *Synaphin*) within tSNE projections as shown in (**a**). **d**, Distribution of cells expressing transgenes, which identifies cells that misexpress the PSC determinant, *Foxc.* BTNs (dark green dots; *n* = 21), PSCs (red dots; n=32), hybrid cells that

express both PSC and BTN marker genes (light blue triangles; n=14), and transformed cells that express PSC markers (blue dots; n=10). The grey dots (n = 10,103) correspond to all dissociated cells that were sequenced in these experiments. **d**, Heatmap of BTNs, PSCs, transformed cells, and hybrid cells showing the relative expression of a select group of genes encoding transcription factors (red), signaling components (green), and cellular effectors (black).

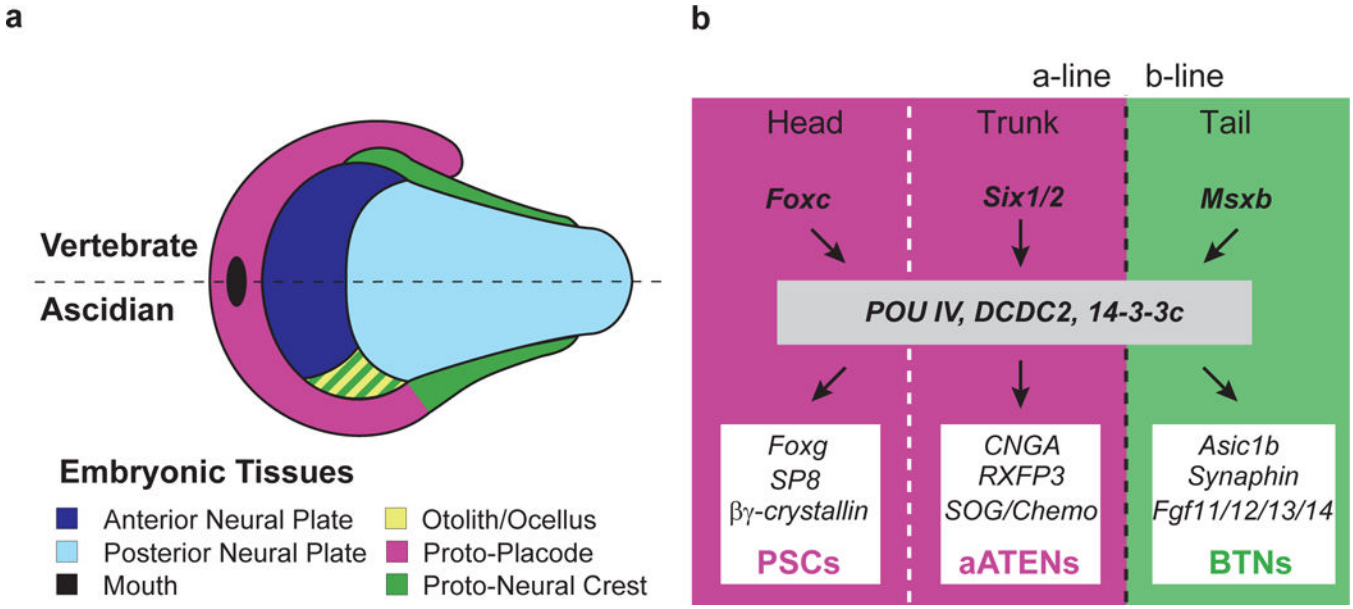

Figure 4 |. Compartmentalization of *Ciona* lateral plate ectoderm.

a, Schematic illustration of the neural plate and its lateral border in vertebrate (top half) and ascidians (bottom half). We proposed that both proto-placode and proto-neural crest evolved from entire lateral plate in the last shared tunicate/vertebrate ancestor. Otolith/ocellus contribution to the proto-neural crest is based on Abitua *et al.*, 2012. **b**, Provisional gene regulatory network for the compartmentalization, specification and differentiation of the lateral plate ectoderm into akin sensory cell types in *Ciona intestinalis*. During early embryogenesis, *Foxc* and *Six1/2* determine the head /trunk boundary (white dotted line) of proto-placode lineages (magenta) while *Msxb* patterns the proto-neural crest territory (green). In tailbud stages, a common developmental program specifies sensory progenitors within each compartment. *CNGA*, *RXFP3* and *SOG/Chemokine-like* expression is based on Abitua *et al.*, 2015[14].